IMTC 2007 – IEEE Instrumentation and Measurement
Technology Conference
Warsaw, Poland, May 1-3, 2007

A Low-Cost Ultra-Wideband Indoor Ranging Technique

A. De Angelis, M. Dionigi, A. Moschitta, P. Carbone
Department of Electronic and Information Engineering, University of Perugia,
via G. Duranti, 93 – 06125 Perugia, Italy.
Phone: +39 075 5853635, Fax: +39 075 5853654
E-mail: {deangelis, dionigi, moschitta, carbone}@diei.unipg.it

Abstract *– This paper presents the development of a low-cost indoor ranging technique based on Time-Of-Arrival (TOA) estimation, using Short-Pulse Ultra-Wideband (UWB) signals. The realized system includes two identical UWB transceiver devices, in which the receiver section is based on a tunnel diode detector and the pulse generation is performed by a common bipolar transistor driven in avalanche mode. An indirect measurement of the distance between the devices is obtained by measuring the frequency of the generated pulse train. A theoretical model of the system is described and a statistical analysis is presented, including the evaluation of the Cramér-Rao Lower Bound ($CRLB$) on the distance estimation. Furthermore the principle of operation of the realized system prototypes is described, along with some implementation issues. Finally experimental results are shown and discussed.*

Keywords *– geolocation, indoor ranging, time-of-flight, ultra-wideband*

I. INTRODUCTION

Recently there has been a growing interest for the research topic of indoor geolocation. The motivation for this interest can be found in many different areas in which an accurate determination of the position of an object in an indoor environment is needed. These range from logistics (asset tracking) to commerce, from medicine to security and defense [1]. Furthermore, an impulse to research in this field is given by the fact that the current widely used systems for global positioning (e.g. GPS) do not provide sufficient coverage for indoor areas. Thus there is a need to extend the capability of such systems and, for specific applications, to obtain a higher degree of accuracy in determining the location. The current state of the art in indoor geolocation includes many different methods used to determine the position of an object or person [2]. Most of them involve measurements of distance from known position nodes, followed by triangulation algorithms. Ultra-Wideband (UWB) signals are potentially good candidates for indoor applications due to their resiliency to multipath phenomena [3].

FCC First Report and Order of 2002 [4], which modifies Part 15 subpart F of the regulation, defines a UWB system as any intentional radiator having a fractional bandwidth greater than 20% or an absolute bandwidth greater than 500 MHz. With such a broad definition, several strategies for generating UWB signals have recently been proposed, like OFDM-UWB or CDMA-UWB, together with the more 'traditional' short-pulse UWB [5]. In our research we adopted the latter technology, which has been investigated to have several advantages for the specific application of indoor geolocation [3][5]. These advantages mainly originate from the fine time resolution of the short pulses, which allows for accurate ranging (in the order of centimeters) and significant reduction of multipath fading.

UWB high data-rate impulse radio communication systems are currently being developed, but they have the drawback of a limited range due to the power restrictions of the FCC regulation. A possible application of such systems can be found in the Wireless Personal Area Network (WPAN) field [6].

Furthermore, UWB low data-rate applications (below a few Mbps) are currently being explored. In this field in fact the main characteristics of short-pulse UWB can be better exploited. Some of these applications include Ground Penetrating Radar (GPR) [7], sensor networks [1] and indoor positioning [5].

In this paper, an RF time-of-arrival-based approach for the distance estimation is proposed. For this application the Short-Pulse UWB technology has been proven to be a good candidate [3][5]. Such an approach might be used as the basis to develop an indoor ranging and positioning system.

II. PROPOSED APPROACH

An indirect measurement of the distance between two transceiver devices may be obtained by measuring the round-trip time-of-flight of an UWB short pulse. This requires high accuracy in time interval measurements, since even a deviation of 1 ns accounts for about 30 cm.

A. Model

Two devices A and B are located at a distance d from each other. One of the devices is initially triggered to transmit a pulse, which is received and retransmitted by the other device. Both systems can receive a pulse and retransmit it after a fixed delay t_A and t_B respectively. In absence of random delays, each of the devices would transmit a periodic train of pulses, with generation frequency

$$f = \frac{1}{\frac{2d}{c} + t_A + t_b} = \frac{1}{T_{RT}}, \qquad (1)$$

$$T_{RT} = \frac{2d}{c} + t_A + t_B,$$

where T_{RT} is the pulse deterministic round trip time. In order to keep into account both the delays introduced by the jitter associated to each node and the random delays introduced by the channel (i.e. multipath phenomena), the round trip time of the n-th transmitted pulse has been defined as

$$T_{RT_n} = \frac{2d}{c} + t_A + t_B + w_n, \tag{2}$$

where w_n is a sequence of independent and identically distributed (i.i.d.) random variables (r.vs), with mean $\eta > 0$ and standard deviation σ such that the probability of the event $\{w_n + t_A + t_B < 0\}$ may be assumed negligible, that is $t_A + t_B + \eta \gg \sigma$. Thus, by assuming that all of the systematic components t_A, t_B and η have been properly determined, and that f is evaluated by measuring with a counter the number $\hat{N}$ of completed round trips in a given time T, the following estimators for the pulse generation frequency f and for the distance d can be obtained

$$\begin{aligned} \hat{f} &= \frac{\hat{N}}{T} \\ \hat{d} &= \frac{c}{2}\left(\frac{T}{\hat{N}} - t_A - t_B - \eta\right) \\ &= \frac{c}{2}\left(\frac{1}{\hat{f}} - t_A - t_B - \eta\right) \end{aligned} \tag{3}$$

In order to assess the statistical efficiency of the proposed approach, the Cramér-Rao Lower Bound $CRLB_d$ and $CRLB_f$ on the estimation of d and f respectively have been evaluated, and compared to simulation results [8]. In particular, under the considered hypotheses, a direct discrete analysis has been carried out, leading to the following results (see the appendix)

$$CRLB_d = \frac{1}{\sum_{n=0}^{N_{MAX}} \frac{(A-B)^2}{\left(\Phi\left(\frac{T-\eta_N}{\sigma_N}\right) - \Phi\left(\frac{T-\eta_{N+1}}{\sigma_{N+1}}\right)\right)}}, \tag{4}$$

with

$$\begin{aligned} A &= -\frac{2N}{c\sigma_N}\varphi\left(\frac{T-\eta_N}{\sigma_N}\right), \\ B &= -\frac{2(N+1)}{c\sigma_{N+1}}\varphi\left(\frac{T-\eta_{N+1}}{\sigma_{N+1}}\right), \\ \varphi(x) &= \frac{1}{\sqrt{2\pi}} e^{-\frac{x^2}{2}}, \\ \Phi(x) &= \int_{-\infty}^{x} \varphi(t)\, dt \end{aligned}$$

and

$$CRLB_f = \frac{4}{c^2\left(\frac{2d}{c} + t_A + t_B + \eta\right)^4} CRLB_d, \tag{5}$$

where $\eta_N = N(t_A + t_B + \eta + 2d/c)$, $\sigma_N = \sigma\sqrt{N}$ and c is the speed of light. Fig. 1 shows the variance of $\hat{f}$ as a function of d, together with the corresponding CRLB, for $c = 3 \cdot 10^8$ m/s, $t_A = t_B = \tau_0 = 1\ \mu$s, $\eta = 0$ s, $\sigma = 6.3$ ns. For each considered distance d, the estimator variance was computed from a set of 10000 simulated measurements. Similarly, Fig. 2 shows the variance of $\hat{d}$ as a function of d, together with the corresponding CRLB, obtained under the same conditions of Fig. 1. It can be observed that in both cases the observed variance is very close to the corresponding CRLB, showing that the proposed estimators are statistically efficient.

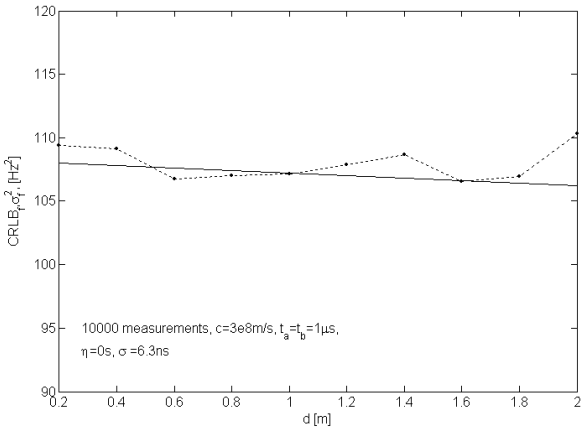

Fig. 1. $CRLB_f$ (continuous line), and variance of the considered estimator (points), obtained from Monte Carlo simulations.

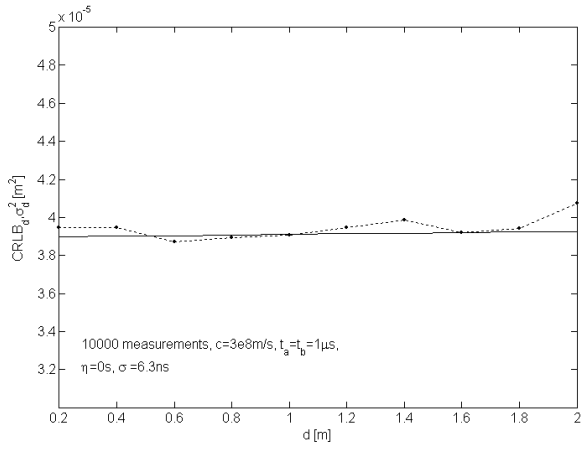

Fig. 2. $CRLB_d$ (continuous line), and variance of the considered estimator (points), obtained from Monte Carlo simulations.

B. Implementation Issues

Two identical prototypes of a transceiver device have been realized and their behavior at various distances has been experimentally observed. The main goal of these initial prototype design has been the usage of low-cost, off-the-shelf components, where possible. A block diagram of the device is shown in Fig. 3. The device's receiver section is based on a tunnel

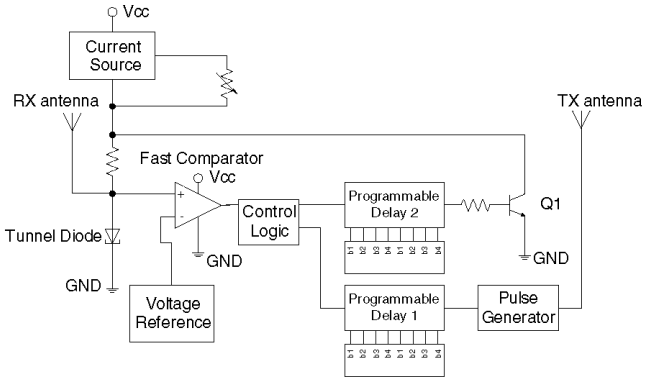

Fig. 3. Block diagram of the prototype device.

diode used as a threshold detector [9][10]. In order to detect an incoming UWB pulse signal received by the antenna, the diode is biased with a constant current near the peak point of the current-voltage characteristic. For the particular model used, 1N3717, the voltage at this bias point is around 50 mV. If the input signal is strong enough, the diode operating point crosses the peak point of the characteristic. Subsequently it enters the unstable negative resistance region and transitions to its 'high-state' (about 500 mV) bias point. The anode is connected to the positive input of a fast comparator with a voltage reference threshold. The voltage change across the tunnel diode causes a rising edge at the comparator output. This is the command signal for the pulse generator, properly delayed by a digital programmable delay IC (n. 1). There is also another delay line (n. 2), whose purpose is to delay the activation of the diode reset transistor. When turned on, this fast-switching npn BJT provides a low impedance path to ground for the current source. The current through the tunnel diode, then, falls below the valley point of the characteristic. Subsequently, when the transistor is turned off, the current flows again through the diode and the component is positioned in its 'low-state' initial bias point. Once the diode is reset, the detection of a subsequent pulse received by the antenna is enabled. Therefore it is important to properly set the two delay values so that the diode does not detect the signal being transmitted by the device itself. In other words, the diode must be disabled until the generated UWB pulse has been transmitted. The sensitivity of the receiver can be adjusted by regulating the diode bias current, while the two delay values can be set through two 8-bit dip-switches connected to the parallel programming ports of the digital delay ICs.

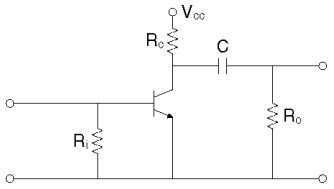

Fig. 4. Pulser schematic.

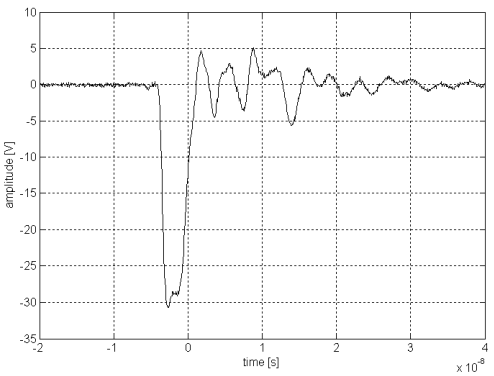

Fig. 5. Measured output pulse, 500 MHz, 1 GSa/s digital oscilloscope.

The pulse generator has been built using a commercial low cost transistor driven in avalanche mode. The pulser circuit is shown in Fig. 4. The high dc feeding voltage (300 V) allows the transistor to switch in avalanche mode once a trigger pulse appears at its base-emitter junction at the terminals of the R_i resistor. When the transistor is driven by the input pulse in the avalanche mode, an abrupt voltage drop at collector-emitter transistor junction appears and it forces the capacitor C to discharge resulting in a negative pulse at R_o terminals. Due to the extremely low resistance of the transistor in avalanche mode a very short time constant of the capacitor discharge is obtained. The stray inductances of the transistor connections remain as the major rise time limiting factor of the circuit. The components values used for this application are the following: $C = 8$ pF, $R_c = 90$ kΩ, $R_o = 50\ \Omega$, $R_i = 50\ \Omega$, while a common BJT NPN transistor 2N3904 has been used. The measured output voltage is shown in Fig. 5. The planar design has reduced the stray inductances and a pulse of 30 V amplitude with rise time of 0.8 ns and fall time of 1.9 ns with small ringing has been observed. Notice that the measuring setup's rise time is $t_r = 0.7$ ns, comparable with the observed rise time.

The prototypes have been realized on single-sided printed circuit boards using surface mount components where possible. Furthermore a ground plane has been used to reduce the effects of interference. The output signal feeds a monopole antenna and the same kind of antenna is used for the receiver section.

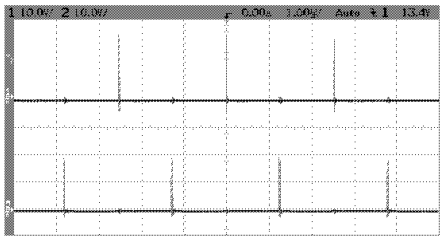

Fig. 6. Signals transmitted by the two prototypes. Each channel is connected to a device's transmission section.

III. RESULTS

In order to verify the behavior of the system, a series of experimental tests has been performed. The pulse train has been qualitatively analyzed by means of a 60 MHz, 200 MSa/s digital oscilloscope and its frequency has been measured using a 225 MHz universal counter. Fig. 6 shows a record of the signals transmitted by the two devices at an approximate distance of 30 cm. By properly programming the delay 1 IC of Fig. 3, the latencies t_A and t_B were set at the same value $\tau_0 \simeq 1.3\ \mu s$, obtaining a frequency of about 383 kHz. Fig. 7a and 7c show the frequency measurement results when the devices (transmitter antennas) are positioned at various known distances, for two different values of the time delay τ_0, about $1.3\ \mu s$ and about $1\ \mu s$ respectively.

For each considered distance, a frequency estimator variance $\sigma_{\hat{f}}^2$ of about 100 Hz^2 was observed. Using such result $\sigma_N \simeq 1.99 \cdot 10^{-6}$ s was obtained, and by substituting such value in (4) and (5), a $CRLB_f$ of 98.04 Hz^2 was calculated, very close to $\sigma_{\hat{f}}^2$. Hence, the proposed frequency estimator appears to be statistically efficient.

As expected, it can be noted that frequency monotonically decreases as distance, and hence time-of-flight, increases. Furthermore, it can be seen from Fig. 7a and 7c that frequency shows an approximately linear behavior. This is consistent with the model described in section II. A. In fact, by neglecting the effect of noise, we have

$$f = \frac{1}{2\tau_0 + \dfrac{2d}{c}} = \frac{1}{2\tau_0 \left(1 + \dfrac{d}{c\tau_0}\right)} \tag{6}$$

Since $\frac{1}{1+x} \simeq (1-x)$ for $x \simeq 0$ and $c\tau_0 \gg d$, from (6) we obtain

$$f \simeq \frac{1}{2\tau_0}\left(1 - \frac{d}{c\tau_0}\right) \tag{7}$$

The negative-slope linear function (7) has a negligible maximum difference from the original curve (6) in the considered system operating range.

To obtain a distance estimation it is possible to use the distance estimator $\hat{d}$ given by (3). However this approach requires the a priori knowledge of both t_A and t_B. Such parameters however cannot be easily estimated, because of the

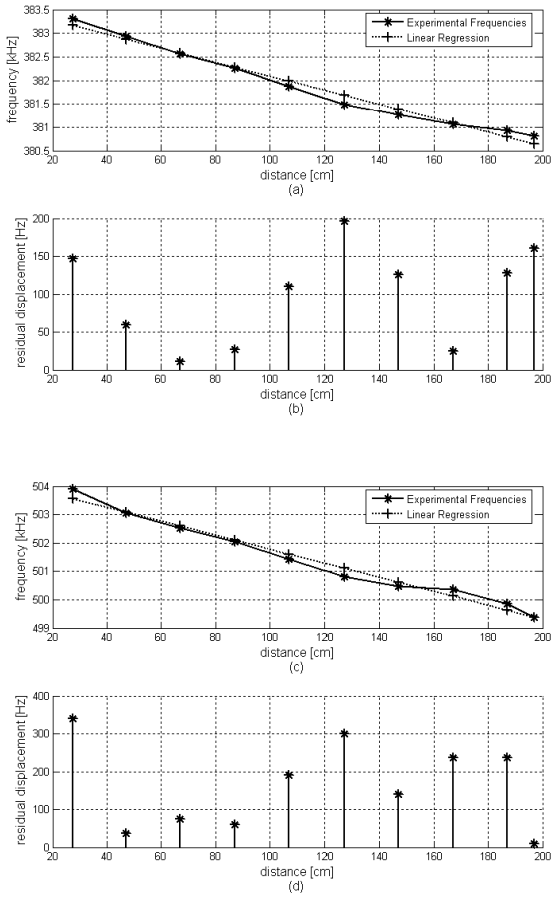

Fig. 7. Measured frequency vs. distance. Each point is the mean of 10 measurement results obtained using a 225 MHz universal counter with 0.1 s gate time.

variations due to temperature, supply voltage and other factors, the analysis of which is difficult. Therefore an approach based on linear regression has been chosen. The linear interpolating function is represented as a dotted line in Fig. 7a and 7c. Fig. 7b and 7d show the corresponding absolute residual deviations. It can also be noted that these deviations display to some extent a common pattern. A possible explanation could be found in near-field effects of the antennas used for the prototypes and in multipath fading effects due to the laboratory environment in which the measurements have been performed. Fig. 8a shows a plot of distance vs experimental frequencies. According to the chosen approach the linear regression function, represented as a dotted line in Fig. 8a, is the distance estimator. Furthermore, Fig. 8b shows the relative deviation of estimated distances. Fig. 9 shows the estimated cumulative distribution function of the relative distance deviation. It is possible to note that with 90% probability the relative deviation is smaller than 10%. Furthermore, the larger values of relative

deviation, about 50%, correspond to the smallest distance considered. As noted before this behavior could be explained by near-field effects of the antennas. In this series of experiments the range is limited to 200 cm because the tests are focused on the analysis and verification of the proposed method.

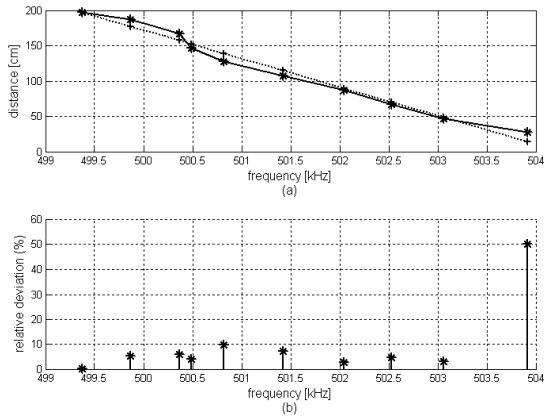

Fig. 8. (a) Distance vs experimental frequencies. The dotted line is the linear regression function. (b) Relative deviation of the estimated distance.

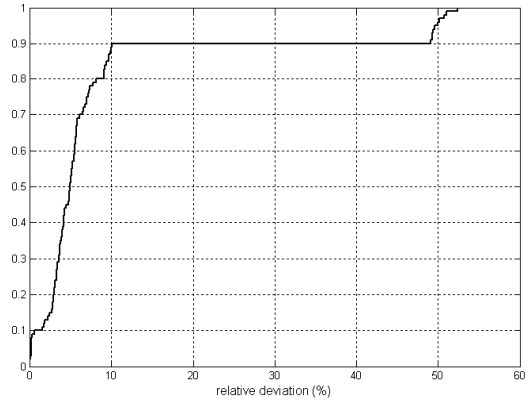

Fig. 9. Estimated cumulative distribution of relative distance deviation.

IV. CONCLUSION

An RF distance measuring system, based on two Short-Pulse Ultra-Wideband transceiver prototypes and a measuring procedure derived from the time-of-arrival approach, has been designed and fully implemented. The performance of the proposed system, which evaluates distances from measurements of the transceiver pulse generation frequency, has been modeled and characterized by means of both simulation and experimental verification. The results show an approximately linear behavior relating the distance to the measured frequency. The Cramér-Rao Lower Bound on the variance of distance estimators has also been evaluated for the considered problem, showing that the proposed approach is statistically efficient. Future developments include a power consumption analysis and optimization of the proposed solution, aimed at developing portable and mobile ranging systems.

Appendix
DERIVATION OF THE CRLB ON THE MEASURED DISTANCE AND FREQUENCY

A. *CRLB on the measured distance*

The CRLB on the distance d, expressed as a function of d, is obtained as the reciprocal of the Fisher information $I_d(d)$, that is [8]:

$$CRLB_d(d) = \frac{1}{I_d(d)},$$

$$\begin{aligned} I_d(d) &= E\left[\left(\frac{\partial \ln P\{m=N;d\}}{\partial d}\right)^2\right] \\ &= \sum_{n=0}^{N_{MAX}} \left(\frac{\partial \ln P\{m=N;d\}}{\partial d}\right)^2 P\{m=N;d\} \\ &= \sum_{n=0}^{N_{MAX}} \frac{1}{P\{m=N;d\}} \left(\frac{\partial P\{m=N;d\}}{\partial d}\right)^2 \end{aligned} \quad \text{(A.1)}$$

where $P\{m=N;d\}$ is the probability of counting N round trips for a given distance d, and N_{MAX} is the maximum number of round trips which may be theoretically completed in the time interval $[0,T]$. The number N_{MAX} is obtained by assuming that no random delays affect the round trips (that is w_n identically equal to zero) and it is given by:

$$N_{MAX} = \left\lfloor \frac{T}{\frac{2d}{c} + t_A + t_B} \right\rfloor \quad \text{(A.2)}$$

where $\lfloor x \rfloor$ is the nearest integer lower than or equal to x. Notice that, by defining the following i.i.d. r.vs

$$r_n = \frac{2d}{c} + t_A + t_B + w_n, \quad r_n > 0 \quad \forall n, \quad \text{(A.3)}$$

the random time T_N needed to complete N round trips is

$$T_N = T_{N-1} + r_N = \sum_{n=0}^{N} r_n, \quad 0 \le T_1 \le \cdots \le T_N, \quad \forall N, \quad \text{(A.4)}$$

which, according to the Central Limit Theorem, may be approximated by a Gaussian r.v., with mean

$$\eta_N = N\left(\frac{2d}{c} + t_A + t_B + \eta\right)$$

and standard deviation

$$\sigma_n = \sigma\sqrt{N},$$

that is its probability density function is

$$f_{T_N}(T_N) = \varphi\left(\frac{T_N - \eta_N}{\sigma_N}\right) \tag{A.5}$$

Moreover, the probability $P\{m = N; d\}$ is the probability $P\{T_N \leq T, T_{N+1} > T\}$ of the joint events $\{T_N \leq T\}$ and $\{T_{N+1} > T\}$ [11]. Notice that (A.4) is a supermartingale sequence of r.vs, and that evaluating the joint probability distribution of T_N and T_{N+1} may lead to complicated recursive expressions [12]. However, by using set theory-based considerations, it can be shown that

$$\begin{aligned} &P\{T_N \leq T, T_{N+1} > T\} = \\ &= P\{T_N \leq T\} - P\{T_N \leq T, T_{N+1} \leq T\} \\ &= P\{T_N \leq T\} - P\{T_{N+1} \leq T\} \end{aligned} \tag{A.6}$$

where the last equality holds because $\{T_{N+1} \leq T\}$ implies $\{T_N \leq T\}$, due to the constraint $0 \leq T_N \leq T_{N+1}$ [11]. Thus, we obtain

$$\begin{aligned} P\{m = N; d\} &= P\{T_N \leq T\} - P\{T_{N+1} \leq T\} \\ &= \Phi\left(\tfrac{T-\eta_N}{\sigma_N}\right) - \Phi\left(\tfrac{T-\eta_{N+1}}{\sigma_{N+1}}\right) \end{aligned} \tag{A.7}$$

Thus, by substituting (A.7) in (A.1), (4) is obtained.

B. CRLB on the measured frequency

The CRLB on the measured frequency can easily be obtained by recalling that, in absence of random delays, the pulse generation frequency f is the reciprocal of the systematic component of the round trip time, which can be expressed as a function of d, that is

$$f(d) = \frac{1}{\frac{2d}{c} + t_A + t_B + \eta} \tag{A.8}$$

Thus, according to [8], $CRLB_f$ may be obtained as

$$CRLB_f = \left(\frac{\partial f(d)}{\partial d}\right)^2 CRLB_d, \tag{A.9}$$

and by differentiating (A.8) with respect to d and substituting the result in (A.9), (5) is obtained.

References

[1] S. Gezici, Z. Tian, G. B. Giannakis, H. Kobayashi, A. F. Molisch, H. V. Poor, and Z. Sahinoglu, "Localization via Ultra-Wideband Radios. A Look at Positioning Aspects for Future Sensor Networks," *IEEE Signal Processing Magazine*, July 2005, pp. 70 - 84.

[2] M. A. Youssef, A. Agrawala, A. U. Shankar "WLAN Location Determination Via Clustering And Probability Distributions," *IEEE Proc. PerCom*, 23-26 March 2003, pp. 143 - 150.

[3] A. F. Molisch, "Ultrawideband Propagation Channels – Theory, Measurement and Modeling," *IEEE Transactions on Vehicular Technology*, Vol. 54, No. 5, September 2005, pp. 1528 - 1545.

[4] "Revision of Part 15 of the Commission's Rules Regarding Ultra-Wideband Transmission Systems," Report and order, adopted February 14, 2002.

[5] R. J. Fontana, "Recent System Applications Of Short-Pulse Ultra-Wideband Technology," *IEEE Transactions on Microwave Theory and Techniques*, Vol. 52, No. 9, September 2004, pp. 2087 - 2104.

[6] T. Terada, S. Yoshizumi, M. Muqsith, Y. Sanada and T. Kuroda, "A CMOS Ultra-Wideband Impulse Radio Transceiver for 1-Mb/s Data Communications and 2.5-cm Range Finding," *IEEE Journal of Solid-State Circuits*, Vol. 41, No. 4, April 2006, pp. 891 - 898.

[7] J. D. Taylor, Editor, *Introduction to Ultra-Wideband Radar Systems*, 1st ed. Boca Ranton, FL: CRC Press, 1995.

[8] S. M. Kay, *Fundamentals of Statistical Signal Processing*, Prentice Hall, 1993.

[9] L. Esaki "Long Journey Into Tunnelling," *Proceedings of the IEEE*, Volume 62, Issue 6, June 1974, pp. 825 - 831. Nobel Prize receiving lecture, 1973.

[10] M. Daniel "Development of Mathematical Models of Semiconductor Devices for CA Analysis," *Proc. IEEE*, Vol. 55, No. 11 , November 1967, pp. 1913 - 1920.

[11] A. Papoulis, *Probability, Random Variables, and Stochastic Processes*, Mc Graw Hill, 1991.

[12] D. Williams, *Probability with Martingales*, Cambridge University Press, 1991.